Supporting Critical Raw Material Circularity – Upcycling Graphite from Waste LIBs to Zn-air Batteries

Reio Praats[a], Alexander Chernyaev[b], Jani Sainio[c], Mari Lundström[b], Ivar Kruusenberg[a] and Kerli Liivand[a]*

[a]R. Praats, I. Kruusenberg, K. Liivand

National Institute of Chemical Physics and Biophysics, Akadeemia tee 23, 12618, Tallinn, Estonia, *E-mail: kerli.liivand@kbfi.ee

[b]A. Chernyaev, M. Lundström

Department of Chemical and Metallurgical Engineering, School of Chemical Engineering, Aalto University, P.O. Box 16200, 00076 Aalto, Finland

[c]J. Sainio

Department of Applied Physics, School of Science, Aalto University, P.O. Box 15100, 00076 Aalto, Finland

Figures

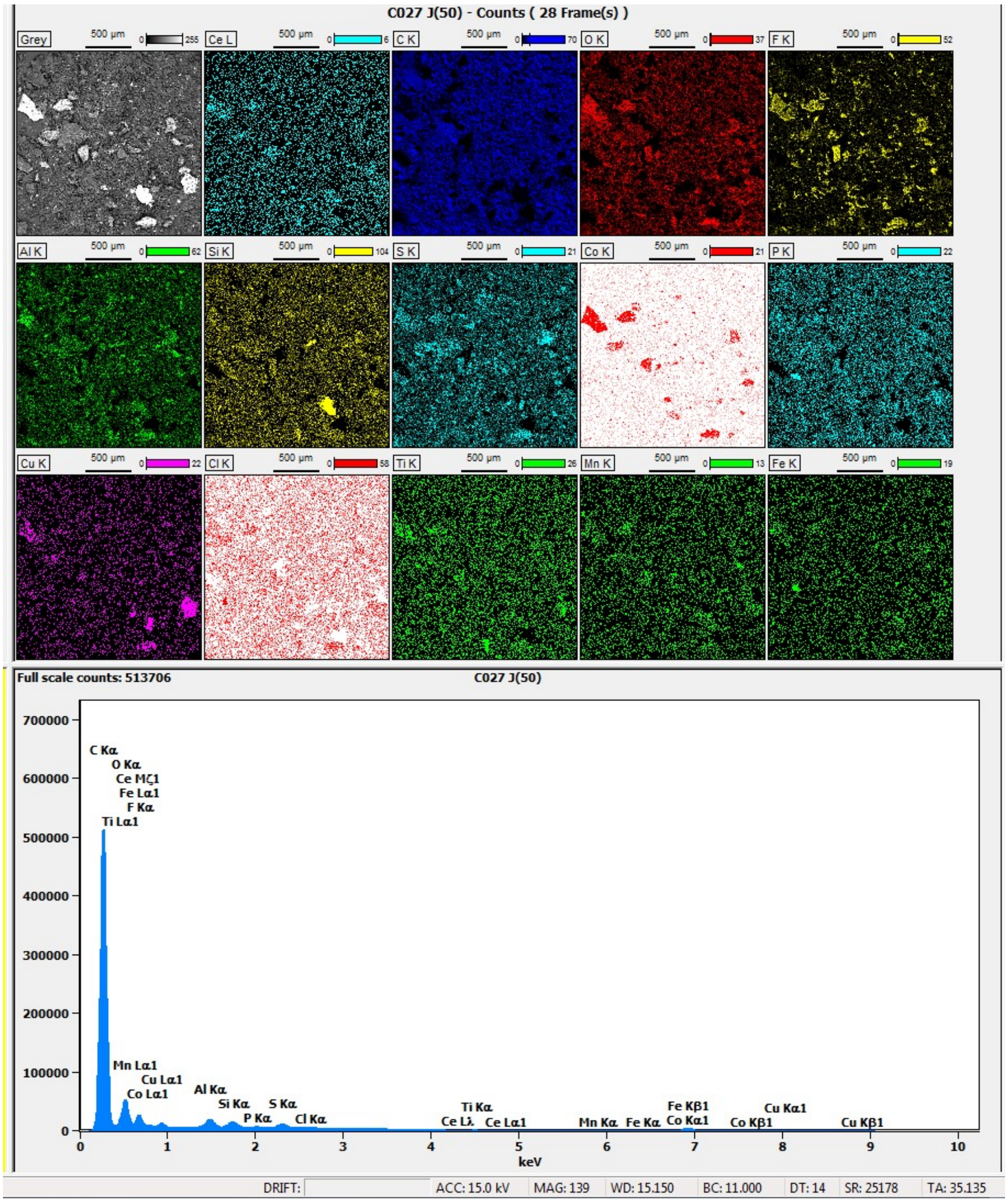

Figure S1. SEM-EDX mapping of Raw material, wt% of elemental composition shown in Table 1 (in manuscript file).

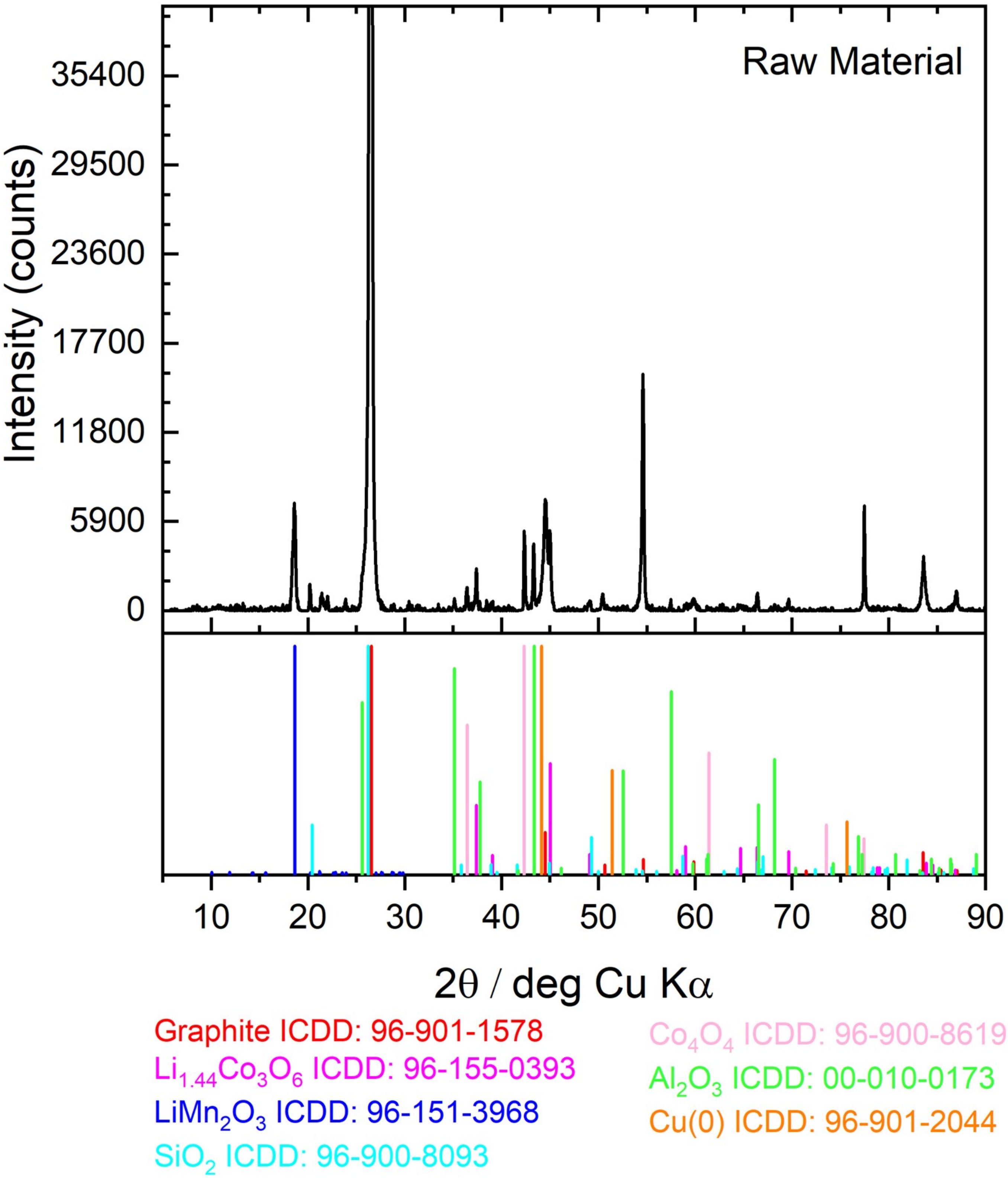

Figure S2. XRD diffractogram of Raw material.

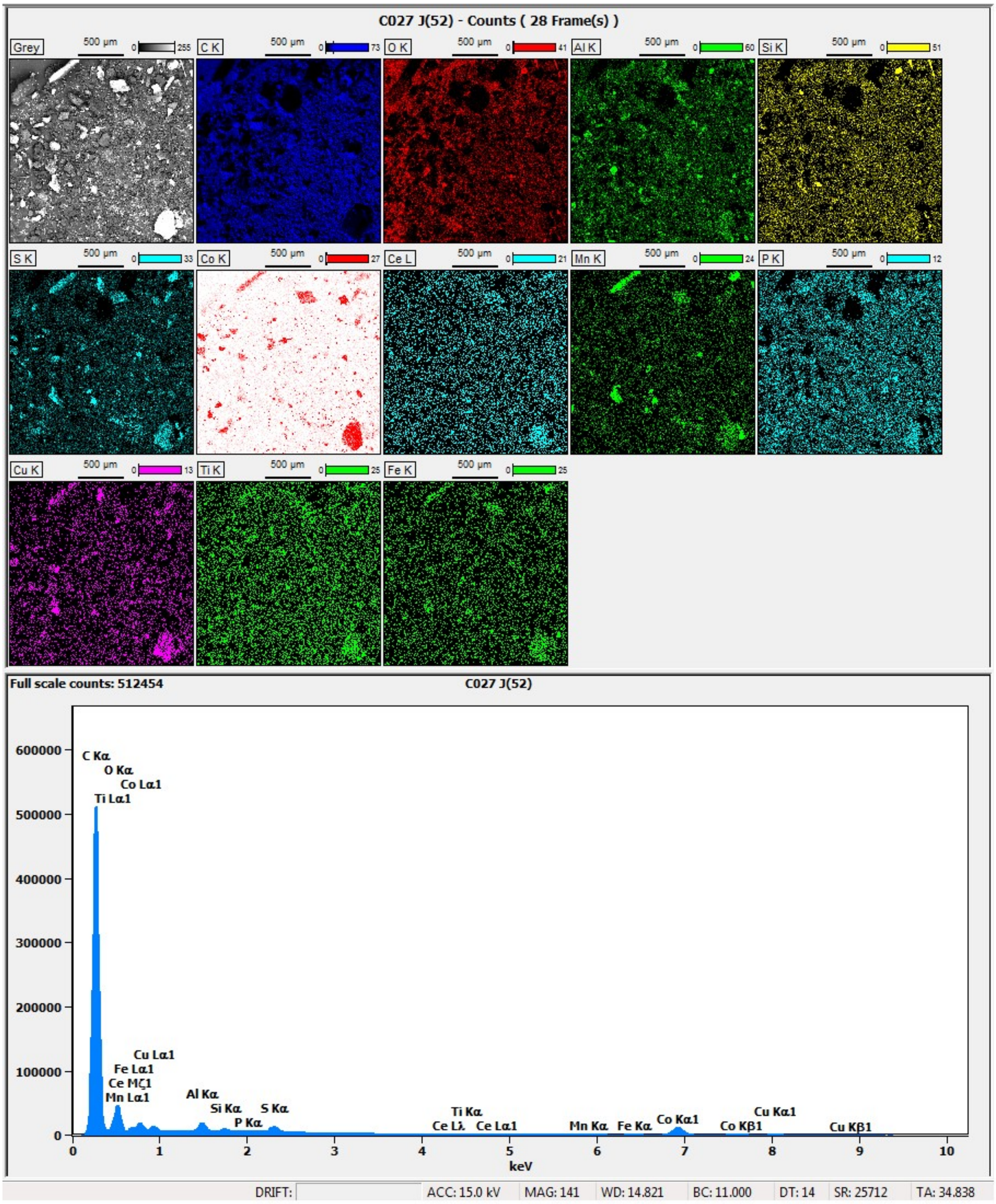

Figure S3. SEM-EDX mapping of *HT-Bat-res*.

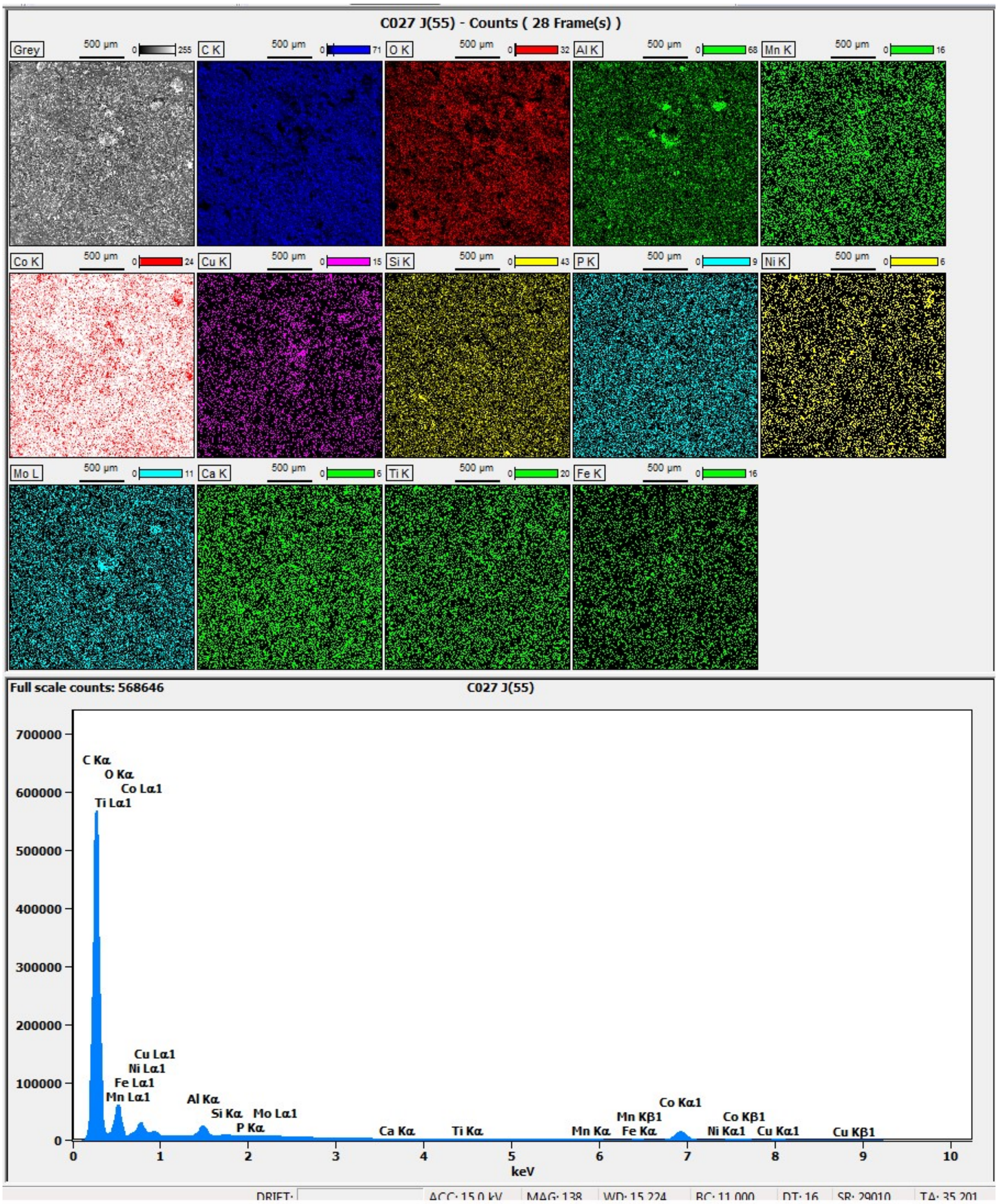

Figure S4. SEM-EDX mapping of *Bat-res-N*.

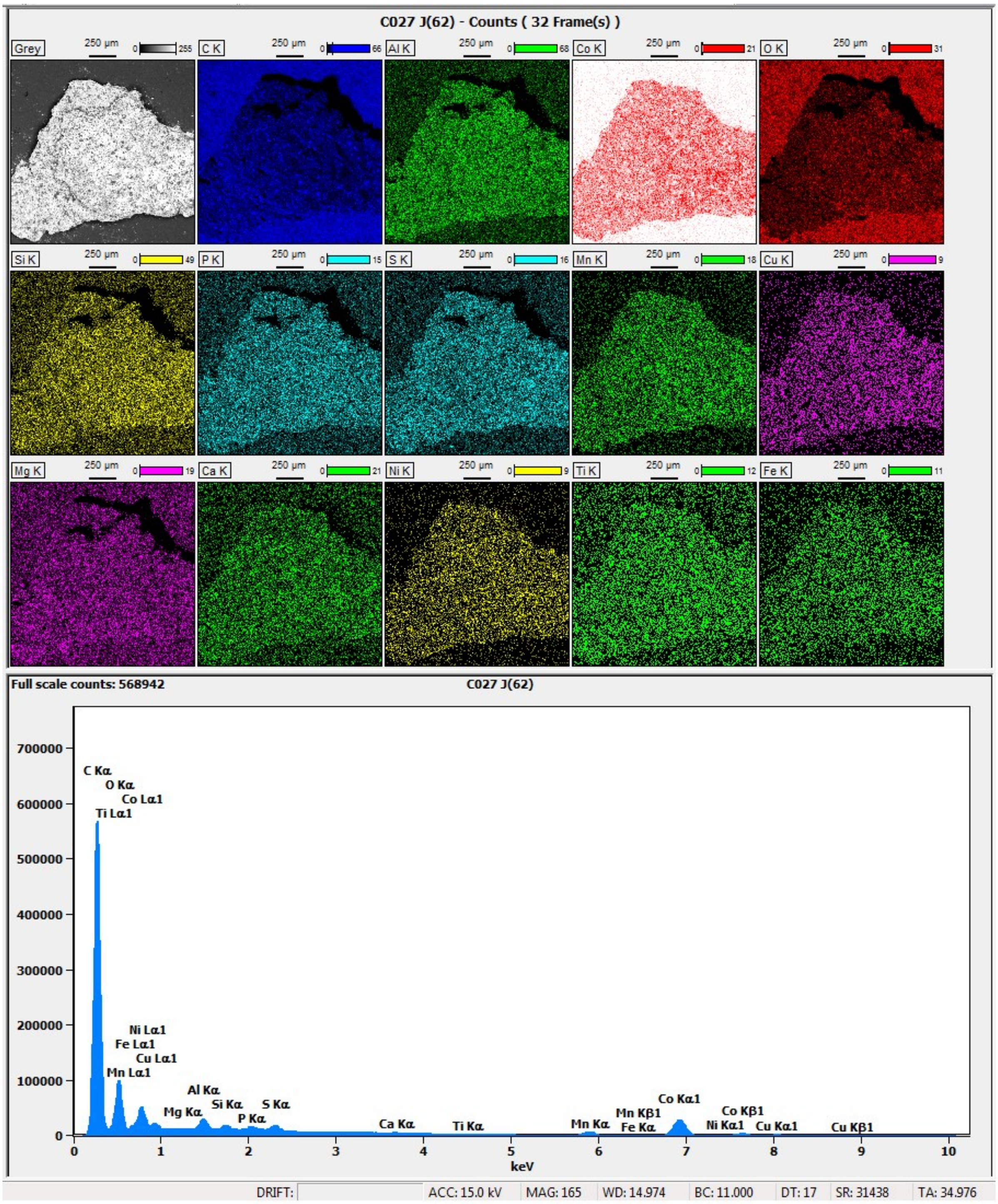

Figure S5. SEM-EDX mapping of *HT-Bat-res-BM-N*.

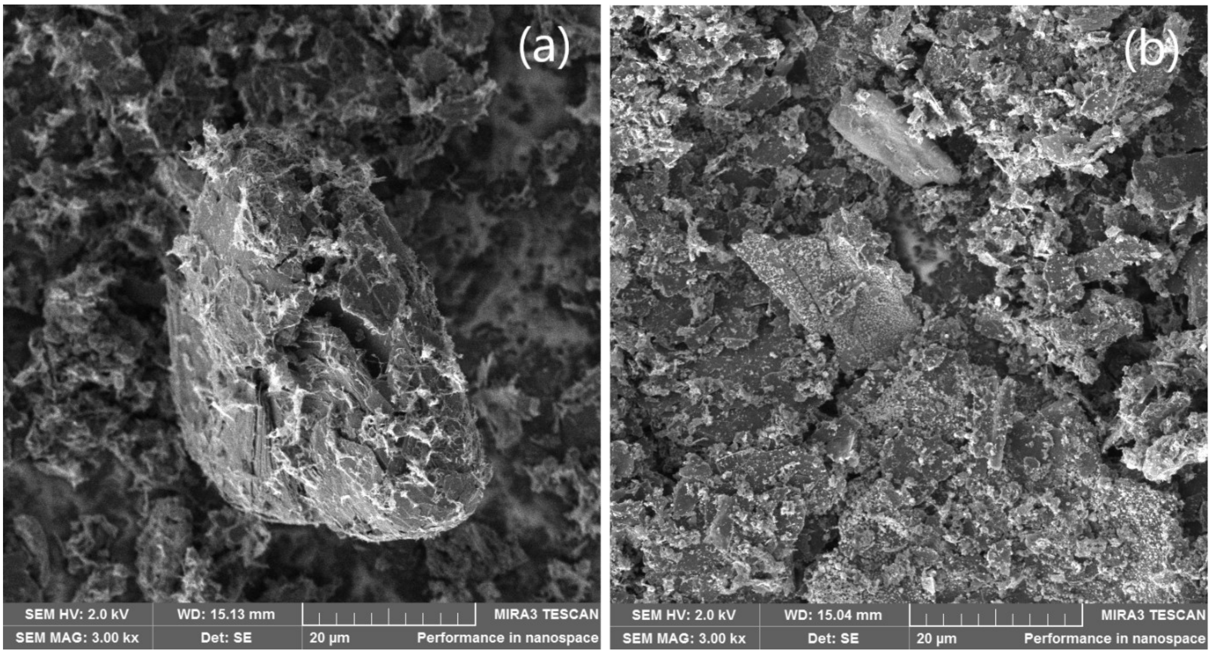

Figure S6. SEM micrographs of (a) *Bat-res-N* and (b) *HT-Bat-res-BM-N* catalyst materials using 3000x magnification.

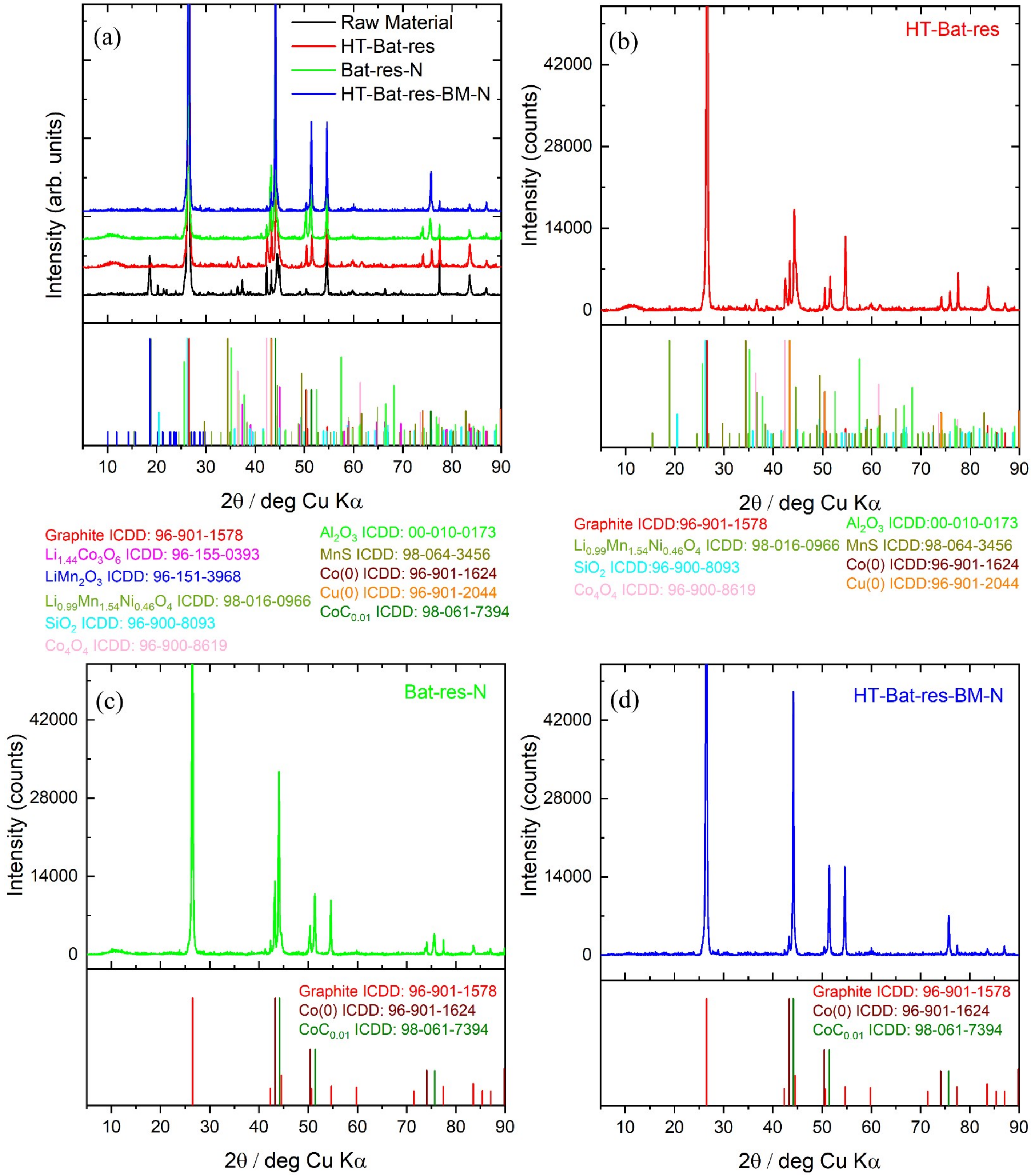

Figure S7. XRD diffractograms of (a) Raw material, *HT-Bat-res*, *Bat-res-N*, *HT-Bat-res-BM-N* catalyst materials, (b) *HT-Bat-res*, (c) *Bat-res-N* and (d) *HT-Bat-res-BM-N* with standard cards.

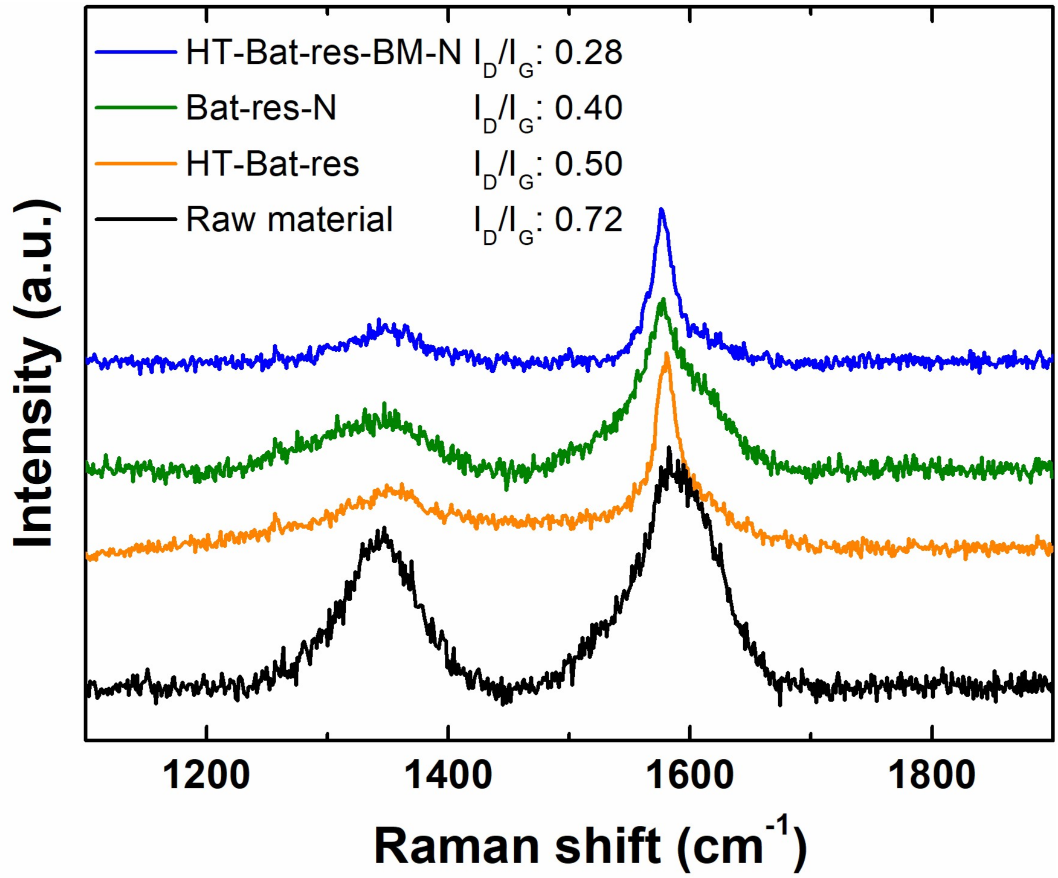

Figure S8. Raman spectra of Raw material, *HT-Bat-res*, *Bat-res-N*, *HT-Bat-res-BM-N* catalyst materials.

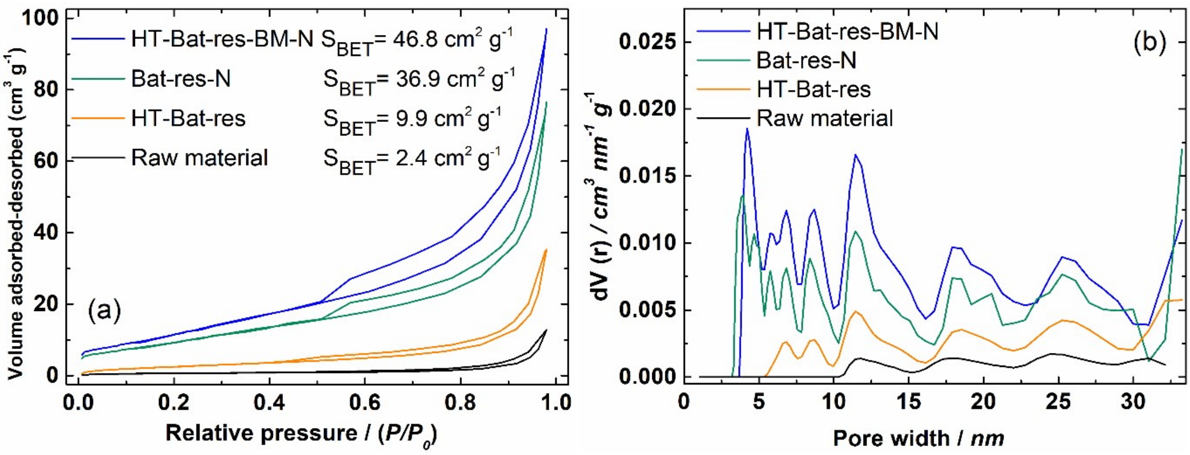

Figure S9. (a) N_2 adsorption-desorption isotherms and (b) pore size distribution of Raw material, *HT-Bat-res*, *Bat-res-N*, *HT-Bat-res-BM-N* materials.

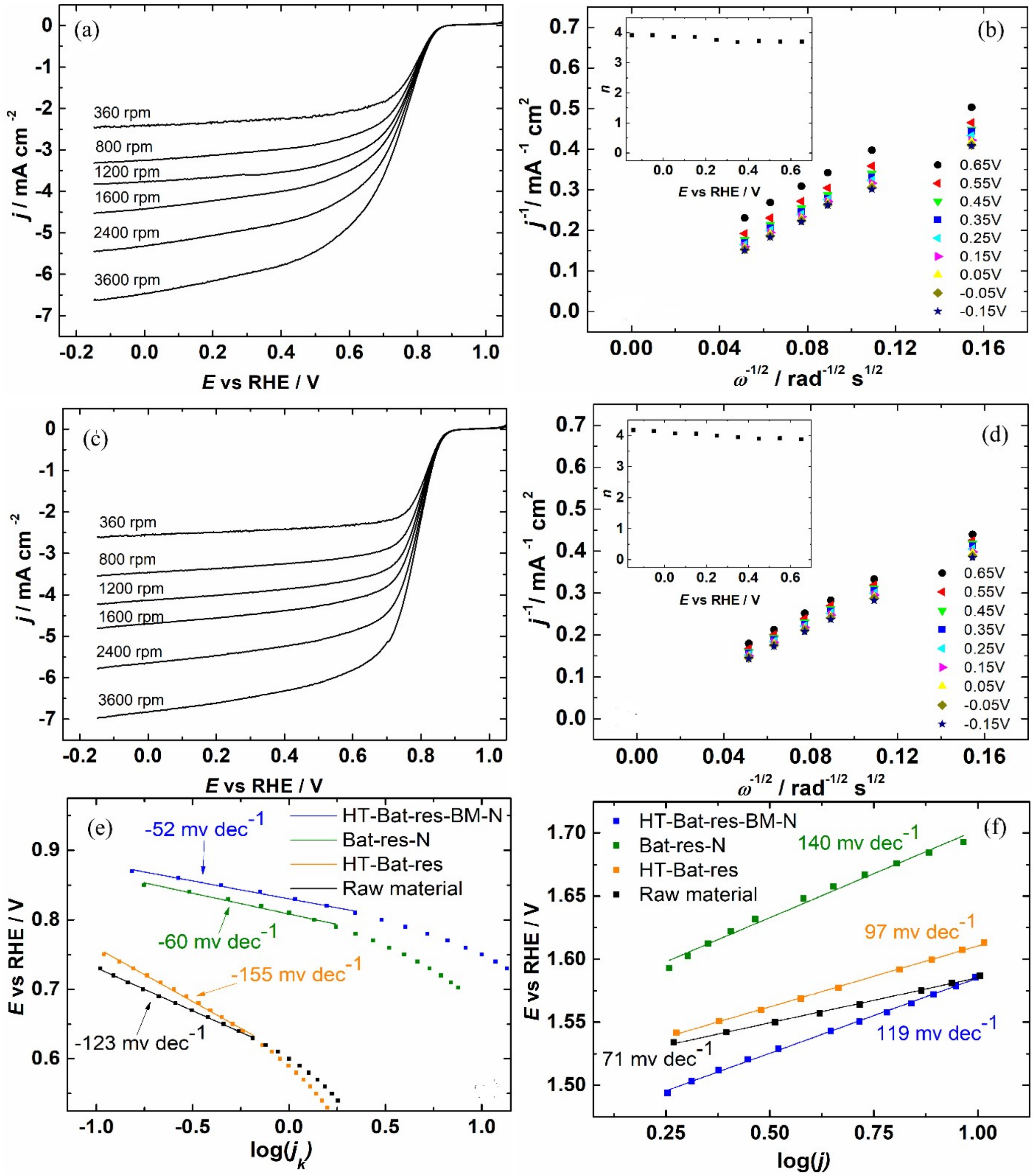

Figure S10. ORR polarization curves on different rotating speeds for (a) *Bat-res-N* and (c) *HT-Bat-res-BM-N* and Koutecky-Levich plots derived from ORR data from the RDE data (b) *Bat-res-N* and (d) *HT-Bat-res-BM-N* for studied materials. The insets of Fig b and d show the dependence of *n* vs potential. (e) ORR Tafel plots and (f) OER Tafel plots for Raw material, *HT-Bat-res*, *Bat-res-N* and *HT-Bat-res-BM-N*.

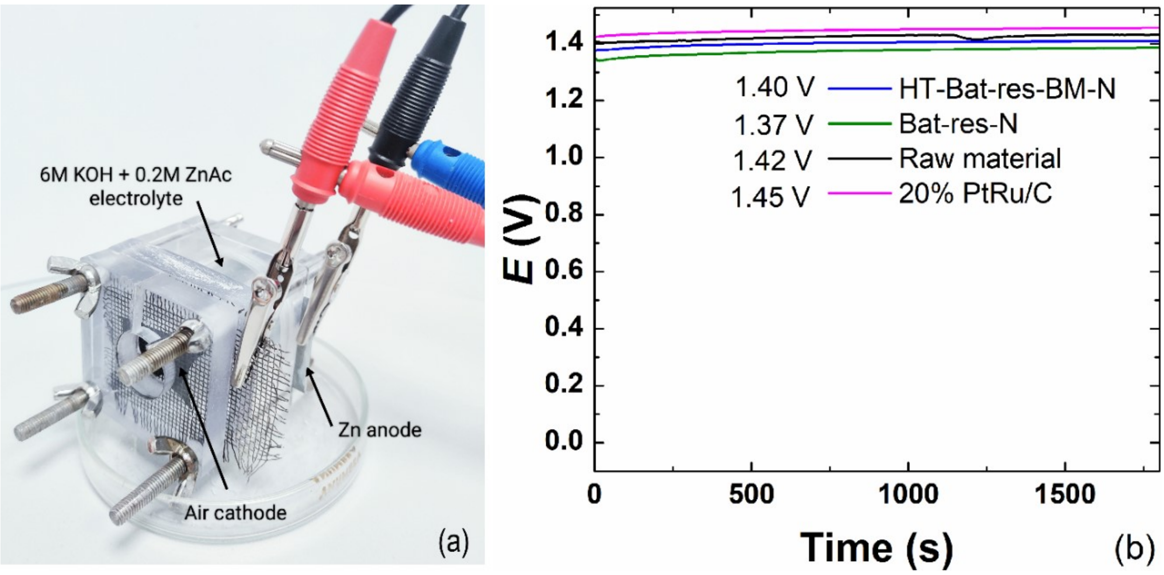

Figure S11. a) Zn-Air battery assembly and b) open circuit potential of different ZABs

Tables

Table S1. The atomic percentages (at-%) of the elements for *Bat-res-N* and *HT-Bat-res-BM-N* samples including peak fitting results from XPS data (data acquired from Fig. 2). The error associated with each value is roughly ±10% of the value.

Element		Bat-res-N	HT-Bat-res-BM-N
C		**77.1**	**74.2**
of which	sp^2 C	57 %	55 %
	sp^3 C / sp^2 C-N	21 %	24 %
	C-O/ sp^3 C-N	9 %	10 %
	C=O	4 %	4 %
	O-C=O	3 %	2 %
	π-π*	6 %	5 %
O		**12.4**	**13.9**
N		**5.6**	**6.4**
of which	Pyridinic-N	50 %	55 %
	Pyrrolic-N	29 %	24 %
	Graphitic-N	11 %	11 %
	N-oxide	10 %	9 %
Al		**2.1**	**2.1**
Mn		**0.5**	**0.9**
Li		**1.4**	**0.6**
Co		**0.1**	**0.4**
of which	Co(0)	6 %	8 %
	CoO / Co-N	94 %	92 %
Zr		**-**	**0.2**
Cu		**0.3**	**0.2**
Ni		**0.1**	**0.1**
F		**0.3**	**0.9**
S		**0.1**	**0.1**

Table S2. Comparison of catalysts ZAB performance.

Catalyst	Mass loading (mg cm^{-2})	OCV (V)	Peak power density (mW cm^{-2})	*j* of peak power density (mA cm^{-2})	Stability (h)	Stability conditions	Ref
Bat-res-N	1.0	1.37	97	150	-	-	This article
HT-Bat-res-N	1.0	1.40	104	160	80	30 min charge-discharge 10 mA cm^{-2}	This article
20% PtRu/C	1.0	1.45	95	158	15	30 min charge-discharge 10 mA cm^{-2}	This article
Co@$CoFe_{0.01}$-N-C	1.0	1.56	174	235	100	10 min charge-discharge 1 mA cm^{-2}	[1]
FeNi/N-GPCM	N/I	1.47	321	450	400	10 min charge-discharge 10 mA cm^{-2}	[2]
$Mn_{0.9}Fe_{2.1}C$/NC	2.0	1.50	160	250	334	20 min charge-discharge 5 mA cm^{-2}	[3]
Pd_3Cu_1/N-rGO	-	1.46	164	230	-	-	[4]
$NiCo_2O_4$/NCNTs/NiCo	~6	1.51	91	175	586	60 min charge-discharge 2 mA cm^{-2}	[5]
FeCo@PCNF	2.0	1.48	290	460	N/I	N/I	[6]
Cu/Fe-NG	1.0	1.53	164	270	18	20 min charge-discharge 10 mA cm^{-2}	[7]
Fe–Cu–N4/C	2.0	1.45	85	150	250 cycles	N/I	[8]
NCNT/MnO–$(MnFe)_2O_3$	2.0	1.45	98	160	20	5 min charge-discharge 20 mA cm^{-2}	[9]
NCNT/CoFe–$CoFe_2O_4$	2.0	1.56	98	160	20	5 min charge-discharge 20 mA cm^{-2}	[9]
$FeCu_{0.3}$-N/C	1.0	1.50	111	200	75	N/I min charge-discharge 5 mA cm^{-2}	[10]
Pd–Cu/C		1.43	219	300	N/I	N/I	[11]

References

1 R. Hao, J. Chen, Z. Wang, Y. Huang, P. Liu, J. Yan, K. Liu, C. Liu and Z. Lu, J. Colloid Interface Sci, 2021, 586, 621–629.
2 M. Zhang, X. M. Hu, Y. Xin, L. Wang, Z. Zhou, L. Yang, J. Jiang and D. Zhang, Sep. Purif.Technol., 2023, 308, 122974.
3 C. Lin, X. Li, S. S. Shinde, D. H. Kim, X. Song, H. Zhang and J. H. Lee, ACS Appl. Energy Mater., 2019, 2, 1747–1755.
4 H. Chen, L. Bao, C. Ou, H. Wang, Y. Liao, R. Li and H. Liu, Energy Fuels, 2022, 36, 7699–7709.
5 C. Chen, H. Su, L. N. Lu, Y. S. Hong, Y. Chen, K. Xiao, T. Ouyang, Y. Qin and Z. Q. Liu, J. Chem. Eng., 2021, 408, 127814.
6 C. Deng, J. Tan, C. Y. Toe, X. Li, G. Li, X. Jiang, S. Wei, H. Yang, Q. Hu and C. He, J. Mater. Chem. A: Mater., 2022, 10, 17217–17224.
7 L. Xu, Y. Tian, D. Deng, H. Li, D. Zhang, J. Qian, S. Wang, J. Zhang, H. Li and S. Sun, ACS Appl. Mater. Interfaces., 2020, 12, 31340–31350.
8 T. H. Chiang, S. C. Sun and Y. S. Chen, J. Taiwan Inst. Chem. Eng., 2020, 115, 175–186.
9 Q. Qin, P. Li, L. Chen and X. Liu, ACS Appl. Mater. Interfaces, 2018, 10, 39828–39838.

10 B. Wang, L. Xu, G. Liu, Y. Ye, Y. Quan, C. Wang, W. Wei, W. Zhu, C. Xu, H. Li and J. Xia, J. Alloys Compd., 2020, 826, 154152.
11 M. Ma, W. Zhu, Q. Shao, H.
12 Shi, F. Liao, C. Shao and M. Shao, ACS Appl. Nano Mater., 2021, 4, 1478–1484.

Please do not adjust margins